Milky Way Accelerometry via Millisecond Pulsar Timing

David F. Phillips[1,*] Aakash Ravi[2,†] Reza Ebadi[2,3] and Ronald L. Walsworth[2,3,4]

[1]*Harvard-Smithsonian Center for Astrophysics, Cambridge, Massachusetts 02138, USA*
[2]*Quantum Technology Center, University of Maryland, College Park, Maryland 20742, USA*
[3]*Department of Physics, University of Maryland, College Park, Maryland 20742, USA*
[4]*Department of Electrical and Computer Engineering, University of Maryland, College Park, Maryland 20742, USA*

The temporal stability of millisecond pulsars is remarkable, rivaling even some terrestrial atomic clocks at long timescales. Using this property, we show that millisecond pulsars distributed in the galactic neighborhood form an ensemble of accelerometers from which we can directly extract the local galactic acceleration. From pulsar spin period measurements, we demonstrate acceleration sensitivity with about 1σ precision using 117 pulsars. We also present a complementary analysis using orbital periods of 13 binary pulsar systems that eliminates the systematics associated with pulsar braking and results in a local acceleration of $(1.7 \pm 0.5) \times 10^{-10}$ m/s^2 in good agreement with expectations. This work is a first step toward dynamically measuring acceleration gradients that will eventually inform us about the dark matter density distribution in the Milky Way galaxy.

Introduction.—Stellar accelerations [1,2] were recently proposed as a promising alternative to kinematic observables in astrophysical characterizations of the dark matter distribution in the Milky Way galaxy. A key feature of such an acceleration-based approach is that it does not require the condition of dynamical equilibrium in the galaxy, an assumption that is inconsistent with the evidence of disequilibria from astronomical surveys [3–17].

Here, we present a complementary approach to Milky Way accelerometry based on long-term monitoring of the differential timing of electromagnetic emissions from an ensemble of millisecond pulsars. The temporal stability of millisecond pulsars—both due to their rotation ("spin") and orbital motion (for binary pulsar systems)—makes them very good astronomical clocks [18]. This property has been useful for a variety of avenues of research [19], including tests of general relativity [20–24], gravitational wave detection [25–33], characterizations of dark matter candidates such as massive gravitons [34–36], primordial black holes [37–40], and ultralight scalar fields [41–49]. In addition, pulsar timing has been used to search for dark matter substructures [50–54] in the galaxy such as minihalos.

Analysis framework.—Here we present two analyses of the local acceleration as obtained from pulsar timing measurements. The first is based on pulsar spin periods and gives an acceleration of $(5.2 \pm 1.6) \times 10^{-10}$ m/s^2, a value that lies within 2σ of the expected acceleration. The second is derived from binary pulsar orbital periods and gives an acceleration of $(1.7 \pm 0.5) \times 10^{-10}$ m/s^2.

We begin by analyzing the pulsar observed spin period P, a quantity that depends on the pulsar's relative velocity with respect to the observer. In turn, the change of the observed spin period with time, $\dot{P}$, depends on the relative acceleration of the pulsar and observer, among other quantities. The apparent acceleration a can be related to these quantities [55–57] via

$$a \equiv c\dot{P}/P - \mu^2 D = \Delta\vec{a}_{\text{gal}} \cdot \hat{u} + a_{\text{br}}, \qquad (1)$$

where c is the speed of light, μ is the total proper motion, and D is the distance from the solar system barycenter (SSB) to the pulsar. In other words, a is the apparent acceleration obtained from the timing $c\dot{P}/P$ corrected for perspective acceleration arising from the motion of the pulsar in the plane of the sky (known as the Shklovskii effect [58] in the pulsar community). Two components comprise a. First is the relative galactic acceleration of the pulsar with respect to the SSB, $\Delta\vec{a}_{\text{gal}}$, projected onto the line of sight, $\hat{u}$, where $\hat{u}$ is a unit vector pointing from the SSB to the pulsar. The second contribution to a, denoted as a_{br}, is the natural braking, or spin-down, of the pulsar rotation due to the emission of electromagnetic radiation [59].

Though the galactic term $\Delta\vec{a}_{\text{gal}}$ is the one of interest for Milky Way accelerometry, it cannot be separated from the braking contribution for an individual pulsar without additional information. However, with an ensemble of pulsars, we can statistically separate the two contributions if we treat the galactic contribution as a deterministic variable resulting from the galactic gravitational potential and the braking acceleration as a random variable drawn from some probability distribution set by pulsar physics [60]. Here, we assume that this braking distribution applies

to all pulsars in our ensemble and, more generally, is the same throughout the galaxy.

In binary millisecond pulsar systems, a similar analysis to that developed for the spin period P can be applied to the orbital period P_b [55]. However, whereas the spin period decays due to the emission of electromagnetic radiation, the orbital period decays due to the emission of gravitational radiation. Fortunately, the change in orbital period due to gravitational waves can be determined directly if there is additional knowledge of the constituent masses M_1, M_2 and the orbital eccentricity e [61]. Similar to Eq. (1), the apparent acceleration can be written as

$$a_b \equiv c\dot{P}_b/P_b - \mu^2 D - a_{GW} = \Delta\vec{a}_{gal} \cdot \hat{u}, \qquad (2)$$

where a_{GW}, the contribution from the orbital period decay as the system emits gravitational waves, appears on the left-hand side of the equation because it can be evaluated precisely for well-characterized pulsars, eliminating uncertainties associated with the spin period method (see the Supplemental Material [62] for more details).

We adopt a simple model [55,57] for the galactic contribution to the apparent acceleration:

$$\Delta\vec{a}_{gal} \cdot \hat{u} \approx a_0 f(D, l, b), \qquad (3a)$$

$$f(D, l, b) \equiv -\cos b \left(\cos l + \frac{\beta}{\sin^2 l + \beta^2} \right), \qquad (3b)$$

where a_0 is the component of the SSB galactic acceleration toward the Galactic Center (GC) and f is a function of the pulsar distance D, galactic longitude l, and latitude b, following the parameterization given in Ref. [55]. The quantity β is given by $\beta = (D/r_0)\cos b - \cos l$, where $r_0 = 8.1$ kpc is the SSB galactocentric radius. Here, we consider only planar galactic accelerations and neglect vertical accelerations, a choice we will justify below. We further assume a flat galactic rotation curve. As shown in the inset of Fig. 1(b), the galactic rotation curve, inferred from diverse astronomical observations [80], deviates from flatness only within a few kpc of the GC; very few pulsars have been characterized in this region, enabling us to use the flat galactic rotation curve approximation.

For this model and assumptions, the apparent acceleration a is linear in the pulsar position function f, with the slope giving the local galactic acceleration a_0. Note that this framework could be straightforwardly extended to study deviations from linearity, which could inform us about the local dark matter density and its distribution in the galaxy [81].

Spin period analysis.—Our pulsar timing data is sourced from the Australian Telescope National Facility pulsar catalog [82]. We select pulsars satisfying the following criteria: (1) Period $P < 10$ ms. (2) Measured total proper motion, μ. (3) Pulsar is not in a globular cluster. Criterion 1
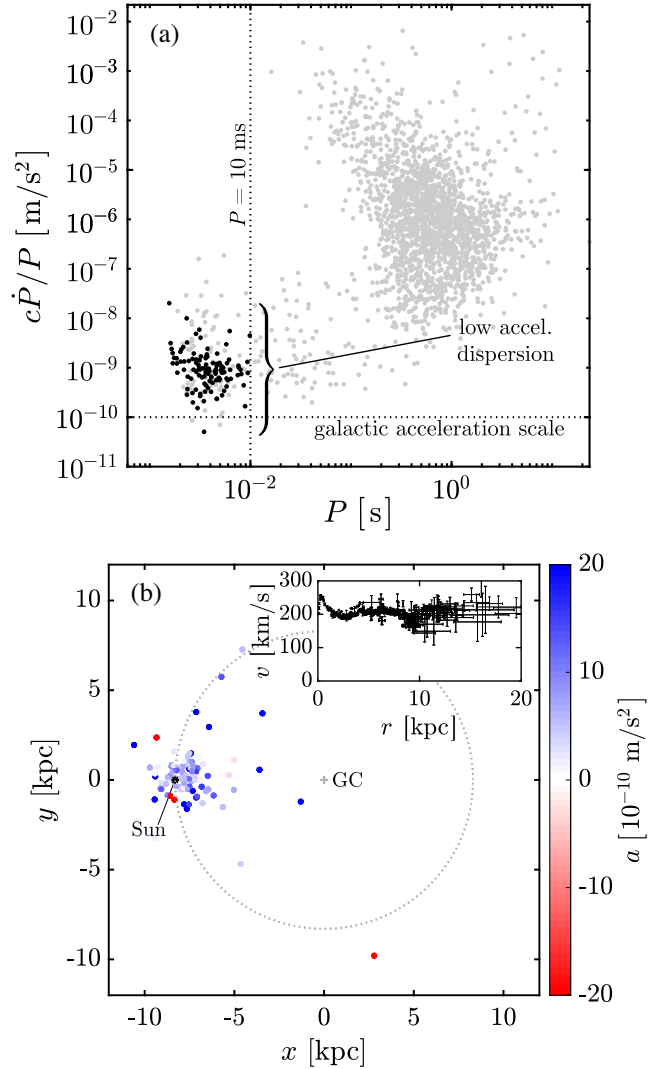

FIG. 1. (a) Apparent pulsar acceleration ($c\dot{P}/P$) distribution vs spin period P. We plot $c\dot{P}/P$ uncorrected for proper motion and visualize the entire pulsar catalog. The pulsars selected for this work are in black in the bottom left of the plot. (b) Spatial distribution of selected pulsars across the galactic midplane, color coded by acceleration. The GC is marked with a cross (+). Pulsar distance uncertainties are suppressed for clarity. Inset: galactic rotation curve with data from Ref. [80].

provides a conservative basis for selecting millisecond pulsars; we choose this subset of all pulsars due to their lower acceleration dispersion as seen in panel (a) of Fig. 1 and their greater age compared to more slowly rotating pulsars. Below, we describe the results of relaxing this constraint. Criterion 2 enables proper motion corrections to pulsar accelerations. These can be as large or larger than the galactic contribution of interest here. Criterion 3 ensures that globular cluster dynamics are not confused with galactic dynamics. The selected pulsar sample is shown in Fig. 1. A total of 117 pulsars satisfy all our criteria. The inset of panel (b), which shows the galactic

rotation curve data from Ref. [80], justifies our flat rotation curve assumption.

Using information from the pulsar catalog, we prepare a vs f data for fitting as described in the Supplemental Material [62]. We employ a Bayesian mixture model [62] to extract the local galactic acceleration a_0 and the braking distribution. The mixture model is capable of handling statistical outliers, and in practice, it rejects approximately 10% of the pulsars in our sample. See Table I of [62] for the outlier scores. The braking distribution is modeled as a Rayleigh distribution with a single parameter λ because of its simplicity and distinct positive skew (a feature observed in the data). Furthermore, it has the property of being supported on only non-negative real numbers, therefore encoding our physical notion that pulsars spin down. The result of our analysis is shown in Fig. 2.

The best-fit estimate for the local galactic acceleration $\hat{a}_0 = (5.2 \pm 1.6) \times 10^{-10}$ m/s² is in tension at the $\sim 2\sigma$ level with $(2.2 \pm 0.1) \times 10^{-10}$ m/s², the value we would expect from a circular velocity of (233 ± 3) km/s [84] at the SSB galactocentric distance of 8.2 kpc [85].
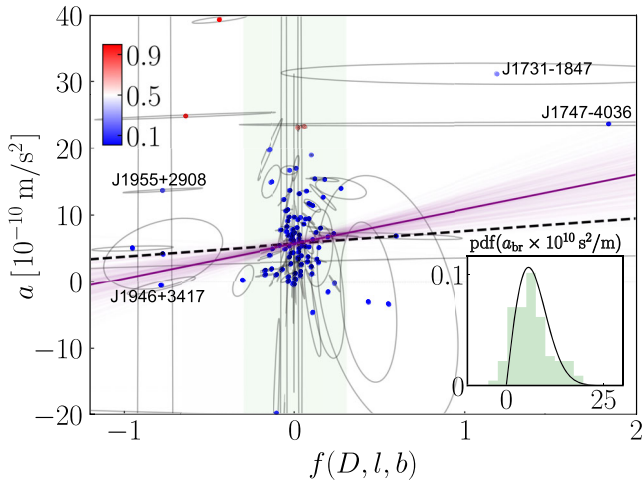

FIG. 2. Local galactic acceleration extracted from pulsar spin periods for selected pulsars. The abscissa $f(D, l, b)$ is a function of pulsar distance D, galactic longitude l, and latitude b [Eq. (3)]. Each dot represents an individual pulsar, and the ellipse around the dot represents the observational covariance matrix for that pulsar. The points are color coded by the degree of certainty that a particular point is an outlier [62]. The thick violet line is the best-fit estimate given by the relationship $a = \hat{a}_0 f + \hat{\lambda}$, where $\hat{a}_0 = (5.2 \pm 1.6) \times 10^{-10}$ m/s² and $\hat{\lambda} = (5.7 \pm 0.4) \times 10^{-10}$ m/s². The fainter violet lines around the thick violet represent the distribution of fitted accelerations [62]. Lastly, the dashed black line has the slope 2.2×10^{-10} m/s², which is the nominal value for the SSB assuming a circular velocity of 233 km/s [83] and galactocentric distance of 8.1 kpc [83]. Inset: recovered braking distribution—in black, the distribution described by $\hat{\lambda}$ is plotted over a histogram of a values for pulsars within the green region $|f| < 0.3$ in (a) that have an outlier score < 0.5. In this region, the braking effect dominates over the galactic component.

This modest disagreement is at least partly driven by the limitations of the existing dataset. The first limitation is that the distribution of pulsars in f is primarily clustered about $f = 0$ with only a few at large $|f|$. The second limitation is that the slope is sensitive to the details of outlier removal. To quantify this sensitivity, we performed a dropout study where we repeated the fit procedure many times, removing a different pulsar from the dataset each time. This analysis revealed that only a handful of pulsars (the four points marked with pulsar alphanumeric identifiers in Fig. 2) have sufficient leverage to change the slope by more than 10%. Of these four pulsars, J1731–1847 has the largest effect. This pulsar is an eclipsing binary system that is susceptible to changes in orbital period as well as dispersion measure [86], thereby reducing the quality of both its timing data and distance estimate. Removing J1731–1847 and the lone pulsar J1747–4036 (which has an extremely large distance uncertainty) results in $\hat{a}_0 \rightarrow (2.5 \pm 2.0) \times 10^{-10}$ m/s², consistent with the expected value from the Milky Way rotation curve. A complete characterization of the properties of all 117 pulsars used in this analysis is beyond the scope of our current work.

The inset in Fig. 2 demonstrates our ability to simultaneously fit the pulsar braking distribution and the galactic acceleration. The black curve is the Rayleigh distribution given by $\hat{\lambda}$, which agrees well with the histogram of pulsar apparent accelerations within the SSB vicinity (i.e., $|f| < 0.3$) that have an outlier score < 0.5. Since the pulsars in the vicinity are co-accelerating with the SSB, the galactic contribution is small compared to the braking contribution, and therefore, these pulsars serve as a test of our model. We stress that the black curve is not a fit to the histogram but is derived from the entire pulsar ensemble and is superimposed on the histogram for comparison. One caveat of note is that the tail of the true braking distribution may be longer than our model suggests. This is because the outlier pruning in the Bayesian mixture model removes pulsars with very large braking values. Thus, the scope of our distribution is limited to only high-Q (quality factor) millisecond pulsars ($a_{br} \lesssim 20 \times 10^{-10}$ m/s²) and does not represent lossy pulsars.

To estimate the effect of vertical accelerations, we use a disk + halo model [87], which gives the vertical component of the galactic acceleration as $a_z = -3.27(1.25\tilde{z}/\sqrt{\tilde{z}^2 + 0.0324} + 0.58\tilde{z}) \times 10^{-11}$ m/s². The symbol $\tilde{z}$ is a dimensionless vertical distance given by z/z_s, and $z_s = 1$ kpc. The vertical contribution to $\Delta\vec{a}_{gal} \cdot \hat{u}$ is $a_z \sin b$, and in most cases, this turns out to be only a few percent of the planar component. We reran the analysis with this component removed and found no appreciable change in the fitted parameters or parameter uncertainties, justifying our neglect of the vertical accelerations.

We also relaxed Criterion 1 to allow all pulsars with $P < 100$ ms and $c\dot{P}/P < 10^{-6}$ m/s² [see Fig. 1(a)] into our sample. This increases our usable number of pulsars by

~25% but has little effect on our parameter estimates or uncertainties.

Looking forward to future surveys of millisecond pulsars, we highlight pulsars within our sample that would benefit from improved measurements in Table I of [62]. We also explore how the acceleration sensitivity σ_{a_0} scales with the number of pulsars N in the sample. A Monte Carlo simulation [62] reveals that with 100 pulsars, our spin period analysis provides sensitivity to the local galactic acceleration at a $\sim 1\sigma$ level (consistent with our fit uncertainties), and we can expect to reach $\sim 3\sigma$ level sensitivity when we have approximately 1,000 pulsars. These extrapolations to larger numbers of pulsars are limited by the biases implicit in the distribution of currently well-characterized pulsars, as well as the unknown distribution of pulsar locations and braking parameters to be observed in the future.

Orbital period analysis.—For our second analysis method, binary millisecond pulsar orbital periods serve as our reference clocks. A summary of the relevant data for the 13 binary pulsars used in our analysis is presented in Table II of the Supplemental Material [62]. In the spin period analysis above, the distribution of intrinsic spin-down rates must be inferred statistically. In contrast, for binary pulsars with well-characterized orbits, we can directly account for the change of the orbital period of
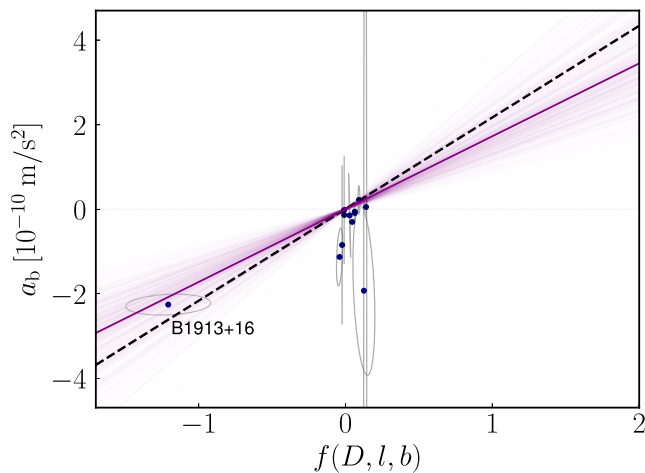

FIG. 3. Local galactic acceleration extracted from binary millisecond pulsar orbital periods given in Table II of Ref. [62]. The abscissa $f(D, l, b)$ is a function of pulsar distance D, galactic longitude l, and latitude b. Each dot represents an individual binary pulsar system, and the ellipse around the dot represents the observational covariance matrix for that system. The thick violet line is the best-fit estimate given by the relationship $a_b = \hat{a}_0 f$, where $\hat{a}_0 = (1.73^{+0.50}_{-0.37}) \times 10^{-10}$ m/s^2. The fainter violet lines around the thick violet represent the distribution of fitted accelerations [62]. Finally, the dashed black line has the slope 2.2×10^{-10} m/s^2, which is the nominal value for the SSB assuming a circular velocity of 233 km/s [83] and galactocentric distance of 8.1 kpc [83].

the pulsar system due to the gravitational wave emissions [61–63]. Once such corrections are applied, the fitting procedure [62] is very similar to the spin periods. The result, as shown in Fig. 3, gives a best-fit estimate for the local galactic acceleration of $\hat{a}_0 = (1.73^{+0.49}_{-0.37}) \times 10^{-10}$ m/s^2. This result is consistent with the expected value from the circular motion assumption, i.e., $(2.2 \pm 0.1) \times 10^{-10}$ m/s^2. Note that the result critically depends on the Hulse-Taylor binary pulsar (B1913 + 16); removing it from the analysis leads to a result for the local acceleration of $(-0.55 \pm 1.3) \times 10^{-10}$ m/s^2, which has a threefold larger uncertainty than the result including this pulsar and differs by about 2σ from the nominally expected value. Additional high-precision measurements of the constituent masses for distant binary pulsar systems will be needed to verify the significance of the present result. Nonetheless, the orbital period analysis is a promising approach, as the explicit compensation for gravitational wave energy loss enables reaching a given acceleration sensitivity with far fewer pulsars than for the spin period analysis. As with spin periods, we highlight pulsars that would benefit from improved measurements in Table II of [62].

Conclusions and outlook.—In summary, we demonstrated two techniques for extracting the acceleration of the SSB in the Milky Way gravitational potential using pulsar timing measurements. These methods are dynamical: they directly access the relative acceleration of pulsars in the galactic neighborhood. Such techniques are complementary to existing kinematic approaches, which currently attain higher precision for the Milky Way gravitational potential but do so with the assumption of dynamical equilibrium. Using spin periods for 117 millisecond pulsars, we reach a sensitivity to the local galactic acceleration with $\sim 1\sigma$ precision but are limited by both the spatial distribution of well-characterized pulsars and the sensitivity to outliers. When high-quality data becomes available for $\sim 1,000$ millisecond pulsars, we expect to reach $\sim 3\sigma$ precision with this approach. Additionally, we show local galactic acceleration sensitivity in agreement (1σ precision) with the nominal value from the galactic rotation curve by analyzing the orbital periods of just 13 binary pulsars. Orbital periods, being unaffected by pulsar braking, offer a cleaner approach to determining the local galactic acceleration.

In the local neighborhood, dark matter comprises approximately 13% of the total density [88]. Thus, under the assumption of a flattened galactic potential, a 3%–4% fractional uncertainty of the local acceleration coupled with improved accuracy in the baryon density (which is only currently known to $\sim 15\%$) are required to achieve 3σ precision on the local dark matter density.

With both the spin and orbital period approaches, additional and improved millisecond pulsar data will provide better galactic acceleration sensitivity, thereby enabling searches for halo substructures [50,89] on the several kpc scale along with deviations from the flat galactic rotation

curve assumed in our current analysis. For example, future releases of GAIA data, including proper motion measurements of pulsar systems and improved distance measurements, could be extremely valuable in extending the reach of the current dataset (see Refs. [90,91] for examples). Additional binary millisecond pulsars characterized by pulsar timing arrays [25,26] will also improve the sensitivity of the orbital period technique. We hope our efforts to determine the galactic gravitational potential dynamically through pulsar timing, as well as characterize the statistical properties of pulsar spin-down rates, will provide motivations for high-precision pulsar astronomy in the future.

After submission of our manuscript, a related paper was posted to the arXiv and subsequently published [95]. This paper reports an analysis of binary pulsar orbital periods similar to the present Letter, with results of comparable precision. The authors also extend the analysis to include vertical accelerations and make estimates of the galactic midplane mass density, the local dark matter density, and the slope of the vertical acceleration profile. Ref. [95] cites our arXiv preprint but incorrectly describes our paper as being limited to spin periods and also mischaracterizes our analysis of the systematic errors associated with the spin period method. Also after submission of our manuscript, the Sun's acceleration in the galaxy was determined to be $(2.32 \pm 0.16) \times 10^{-10}$ m/s^2 [96] using precision GAIA astrometry data for $> 10^6$ compact extragalactic sources. While this measurement is more precise than those reported here, we envision that additional pulsar data will enable us to both improve our precision and probe galactic structure beyond the local acceleration. It is also worth noting that the astrometry-based measurement of the local acceleration has already been combined with binary pulsar orbital period measurements to extract galactic parameters [97], highlighting the complementarity of these approaches.

D. F. P. and A. R. contributed equally to this work.

———————————

[*]Corresponding author.
dphillips@cfa.harvard.edu
[†]Corresponding author.
aakash.ravi@gmail.com

[1] A. Ravi, N. Langellier, D. F. Phillips, M. Buschmann, B. R. Safdi, and R. L. Walsworth, Phys. Rev. Lett. **123,** 091101 (2019).
[2] H. Silverwood and R. Easther, Pub. Astron. Soc. Aust. **36,** e038 (2019).
[3] H. J. Newberg, B. Yanny, C. Rockosi, E. K. Grebel, H.-W. Rix, J. Brinkmann, I. Csabai, G. Hennessy, R. B. Hindsley, R. Ibata et al., Astrophys. J. **569,** 245 (2002).
[4] J. D. Crane, S. R. Majewski, H. J. Rocha-Pinto, P. M. Frinchaboy, M. F. Skrutskie, and D. R. Law, Astrophys. J. Lett. **594,** L119 (2003).
[5] F. A. Gómez, I. Minchev, B. W. O'Shea, Y. S. Lee, T. C. Beers, D. An, J. S. Bullock, C. W. Purcell, and A. Villalobos, Mon. Not. R. Astron. Soc. **423,** 3727 (2012).
[6] L. M. Widrow, S. Gardner, B. Yanny, S. Dodelson, and H.-Y. Chen, Astrophys. J. Lett. **750,** L41 (2012).
[7] F. A. Gómez, I. Minchev, B. W. O'Shea, T. C. Beers, J. S. Bullock, and C. W. Purcell, Mon. Not. R. Astron. Soc. **429,** 159 (2013).
[8] J. L. Carlin, J. DeLaunay, H. J. Newberg, L. Deng, D. Gole, K. Grabowski, G. Jin, C. Liu, X. Liu, A.-L. Luo et al., Astrophys. J. Lett. **777,** L5 (2013).
[9] M. E. K. Williams, M. Steinmetz, J. Binney, A. Siebert, H. Enke, B. Famaey, I. Minchev, R. S. de Jong, C. Boeche, K. C. Freeman et al., Mon. Not. R. Astron. Soc. **436,** 101 (2013).
[10] Y. Xu, H. J. Newberg, J. L. Carlin, C. Liu, L. Deng, J. Li, R. Schönrich, and B. Yanny, Astrophys. J. **801,** 105 (2015).
[11] I. Carrillo, I. Minchev, G. Kordopatis, M. Steinmetz, J. Binney, F. Anders, O. Bienaymé, J. Bland-Hawthorn, B. Famaey, K. C. Freeman et al., Mon. Not. R. Astron. Soc. **475,** 2679 (2018).
[12] R. Schönrich and W. Dehnen, Mon. Not. R. Astron. Soc. **478,** 3809 (2018).
[13] T. Antoja, A. Helmi, M. Romero-Gómez, D. Katz, C. Babusiaux, R. Drimmel, D. W. Evans, F. Figueras, E. Poggio, C. Reylé et al., Nature (London) **561,** 360 (2018).
[14] C. F. P. Laporte, I. Minchev, K. V. Johnston, and F. A. Gómez, Mon. Not. R. Astron. Soc. **485,** 3134 (2019).
[15] M. Bennett and J. Bovy, Mon. Not. R. Astron. Soc. **482,** 1417 (2019).
[16] L. Necib, M. Lisanti, and V. Belokurov, Astrophys. J. **874,** 3 (2019).
[17] L. Necib, B. Ostdiek, M. Lisanti, T. Cohen, M. Freytsis, and S. Garrison-Kimmel, Astrophys. J. **903,** 25 (2020).
[18] J. G. Hartnett and A. N. Luiten, Rev. Mod. Phys. **83,** 1 (2011).
[19] R. N. Manchester, J. Astrophys. Astron. **38,** 42 (2017).
[20] J. M. Weisberg, D. J. Nice, and J. H. Taylor, Astrophys. J. **722,** 1030 (2010).
[21] J. M. Weisberg and Y. Huang, Astrophys. J. **829,** 55 (2016).
[22] S. M. Ransom, I. H. Stairs, A. M. Archibald, J. W. T. Hessels, D. L. Kaplan, M. H. van Kerkwijk, J. Boyles, A. T. Deller, S. Chatterjee, A. Schechtman-Rook et al., Nature (London) **505,** 520 (2014).
[23] A. M. Archibald, N. V. Gusinskaia, J. W. T. Hessels, A. T. Deller, D. L. Kaplan, D. R. Lorimer, R. S. Lynch, S. M. Ransom, and I. H. Stairs, Nature (London) **559,** 73 (2018).

[24] G. Voisin, I. Cognard, P. C. C. Freire, N. Wex, L. Guillemot, G. Desvignes, M. Kramer, and G. Theureau, Astron. Astrophys. **638**, A24 (2020).

[25] A. N. Lommen, Rep. Prog. Phys. **78**, 124901 (2015).

[26] R. M. Shannon, V. Ravi, W. A. Coles, G. Hobbs, M. J. Keith, R. N. Manchester, J. S. B. Wyithe, M. Bailes, N. D. R. Bhat, S. Burke-Spolaor et al., Science **342**, 334 (2013).

[27] R. M. Shannon, V. Ravi, L. T. Lentati, P. D. Lasky, G. Hobbs, M. Kerr, R. N. Manchester, W. A. Coles, Y. Levin, M. Bailes et al., Science **349**, 1522 (2015).

[28] P. B. Demorest, R. D. Ferdman, M. E. Gonzalez, D. Nice, S. Ransom, I. H. Stairs, Z. Arzoumanian, A. Brazier, S. Burke-Spolaor, S. J. Chamberlin et al., Astrophys. J. **762**, 94 (2013).

[29] L. Lentati, S. R. Taylor, C. M. F. Mingarelli, A. Sesana, S. A. Sanidas, A. Vecchio, R. N. Caballero, K. J. Lee, R. van Haasteren, S. Babak et al., Mon. Not. R. Astron. Soc. **453**, 2576 (2015).

[30] S. Babak, A. Petiteau, A. Sesana, P. Brem, P. A. Rosado, S. R. Taylor, A. Lassus, J. W. T. Hessels, C. G. Bassa, M. Burgay et al., Mon. Not. R. Astron. Soc. **455**, 1665 (2016).

[31] Z. Arzoumanian, A. Brazier, S. Burke-Spolaor, S. J. Chamberlin, S. Chatterjee, B. Christy, J. M. Cordes, N. J. Cornish, K. Crowter, P. B. Demorest et al., Astrophys. J. **821**, 13 (2016).

[32] K. Aggarwal, Z. Arzoumanian, P. T. Baker, A. Brazier, M. R. Brinson, P. R. Brook, S. Burke-Spolaor, S. Chatterjee, J. M. Cordes, N. J. Cornish et al., Astrophys. J. **880**, 116 (2019).

[33] J. P. W. Verbiest, L. Lentati, G. Hobbs, R. van Haasteren, P. B. Demorest, G. H. Janssen, J.-B. Wang, G. Desvignes, R. N. Caballero, M. J. Keith et al., Mon. Not. R. Astron. Soc. **458**, 1267 (2016).

[34] S. Dubovsky, P. Tinyakov, and I. Tkachev, Phys. Rev. Lett. **94**, 181102 (2005).

[35] D. Baskaran, A. G. Polnarev, M. S. Pshirkov, and K. A. Postnov, Phys. Rev. D **78**, 044018 (2008).

[36] M. Pshirkov, A. Tuntsov, and K. A. Postnov, Phys. Rev. Lett. **101**, 261101 (2008).

[37] N. Seto and A. Cooray, Astrophys. J. **659**, L33 (2007).

[38] K. Kashiyama and N. Seto, Mon. Not. R. Astron. Soc. **426**, 1369 (2012).

[39] K. Schutz and A. Liu, Phys. Rev. D **95**, 023002 (2017).

[40] J. A. Dror, H. Ramani, T. Trickle, and K. M. Zurek, Phys. Rev. D **100**, 023003 (2019).

[41] A. Khmelnitsky and V. Rubakov, J. Cosmol. Astropart. Phys. 02 (2014) 019.

[42] N. K. Porayko and K. A. Postnov, Phys. Rev. D **90**, 062008 (2014).

[43] P. W. Graham, D. E. Kaplan, J. Mardon, S. Rajendran, and W. A. Terrano, Phys. Rev. D **93**, 075029 (2016).

[44] I. de Martino, T. Broadhurst, S. H. H. Tye, T. Chiueh, H.-Y. Schive, and R. Lazkoz, Phys. Rev. Lett. **119**, 221103 (2017).

[45] I. de Martino, T. Broadhurst, S. H. H. Tye, T. Chiueh, H.-Y. Schive, and R. Lazkoz, Galaxies **6**, 10 (2018).

[46] R.-G. Cai, T.-B. Liu, and S.-J. Wang, Phys. Rev. D **97**, 023027 (2018).

[47] N. K. Porayko, X. Zhu, Y. Levin, L. Hui, G. Hobbs, A. Grudskaya, K. Postnov, M. Bailes, N. D. R. Bhat, W. Coles et al., Phys. Rev. D **98**, 102002 (2018).

[48] A. Caputo, L. Sberna, M. Frias, D. Blas, P. Pani, L. Shao, and W. Yan, Phys. Rev. D **100**, 063515 (2019).

[49] D. Blas, D. Lopez Nacir, and S. Sibiryakov, Phys. Rev. D **101**, 063016 (2020).

[50] E. R. Siegel, M. P. Hertzberg, and J. N. Fry, Mon. Not. R. Astron. Soc. **382**, 879 (2007).

[51] S. Baghram, N. Afshordi, and K. M. Zurek, Phys. Rev. D **84**, 043511 (2011).

[52] H. A. Clark, G. F. Lewis, and P. Scott, Mon. Not. R. Astron. Soc. **456**, 1394 (2016).

[53] H. A. Clark, G. F. Lewis, and P. Scott, Mon. Not. R. Astron. Soc. **456**, 1402 (2016).

[54] H. Ramani, T. Trickle, and K. M. Zurek, J. Cosmol. Astropart. Phys. 12 (2020) 033.

[55] T. Damour and J. H. Taylor, Astrophys. J. **366**, 501 (1991).

[56] E. S. Phinney, Phil. Trans. R. Soc. A **341**, 39 (1992).

[57] D. J. Nice and J. H. Taylor, Astrophys. J. **441**, 429 (1995).

[58] I. S. Shklovskii, Sov. Astron. **13**, 562 (1970), https://ui.adsabs.harvard.edu/abs/1970SvA....13..562S/abstract.

[59] A. Lyne and F. Graham-Smith, Pulsar Astronomy, 4th ed. (Cambridge University Press, Cambridge, England, 2012).

[60] R. X. Xu and G. J. Qiao, Astrophys. J. **561**, L85 (2001).

[61] P. C. Peters and J. Mathews, Phys. Rev. **131**, 435 (1963).

[62] See Supplemental Material, which includes Refs. [21,59, 61,63–79], at http://link.aps.org/supplemental/10.1103/PhysRevLett.126.141103 for details on spin and orbital period analyses.

[63] L. Shao, N. Wex, and S.-Y. Zhou, Phys. Rev. D **102**, 024069 (2020).

[64] D. Foreman-Mackey, D. W. Hogg, D. Lang, and J. Goodman, Publ. Astron. Soc. Pac. **125**, 306 (2013).

[65] J. M. Yao, R. N. Manchester, and N. Wang, Astrophys. J. **835**, 29 (2017).

[66] D. W. Hogg, J. Bovy, and D. Lang, arXiv:1008.4686.

[67] J. Antoniadis, P. C. Freire, N. Wex, T. M. Tauris, R. S. Lynch, M. H. van Kerkwijk, M. Kramer, C. Bassa, V. S. Dhillon, T. Driebe et al., Science **340**, 1233232 (2013).

[68] D. Reardon, G. Hobbs, W. Coles, Y. Levin, M. Keith, M. Bailes, N. Bhat, S. Burke-Spolaor, S. Dai, M. Kerr et al., Mon. Not. R. Astron. Soc. **455**, 1751 (2016).

[69] B. Perera, M. DeCesar, P. Demorest, M. Kerr, L. Lentati, D. Nice, S. Osłowski, S. Ransom, M. Keith, Z. Arzoumanian et al., Mon. Not. R. Astron. Soc. **490**, 4666 (2019).

[70] G. Desvignes, R. Caballero, L. Lentati, J. Verbiest, D. Champion, B. Stappers, G. Janssen, P. Lazarus, S. Osłowski, S. Babak et al., Mon. Not. R. Astron. Soc. **458**, 3341 (2016).

[71] K. Lazaridis, N. Wex, A. Jessner, M. Kramer, B. Stappers, G. Janssen, G. Desvignes, M. Purver, I. Cognard, G. Theureau et al., Mon. Not. R. Astron. Soc. **400**, 805 (2009).

[72] E. Fonseca, I. H. Stairs, and S. E. Thorsett, Astrophys. J. **787**, 82 (2014).

[73] W. Zhu, G. Desvignes, N. Wex, R. Caballero, D. Champion, P. Demorest, J. Ellis, G. Janssen, M. Kramer, A. Krieger et al., Mon. Not. R. Astron. Soc. **482**, 3249 (2019).

[74] P. C. Freire, N. Wex, G. Esposito-Farese, J. P. Verbiest, M. Bailes, B. A. Jacoby, M. Kramer, I. H. Stairs, J. Antoniadis, and G. H. Janssen, Mon. Not. R. Astron. Soc. **423**, 3328 (2012).

[75] R. D. Ferdman, I. H. Stairs, M. Kramer, G. H. Janssen, C. G. Bassa, B. W. Stappers, P. B. Demorest, I. Cognard,

G. Desvignes, G. Theureau *et al.*, Mon. Not. R. Astron. Soc. **443**, 2183 (2014).

[76] J. M. Weisberg, S. Stanimirović, K. Xilouris, A. Hedden, A. de la Fuente, S. B. Anderson, and F. A. Jenet, Astrophys. J. **674**, 286 (2008).

[77] I. Cognard, P. C. Freire, L. Guillemot, G. Theureau, T. M. Tauris, N. Wex, E. Graikou, M. Kramer, B. Stappers, A. G. Lyne *et al.*, Astrophys. J. **844**, 128 (2017).

[78] A. T. Deller, J. M. Weisberg, D. J. Nice, and S. Chatterjee, Astrophys. J. **862**, 139 (2018).

[79] H. T. Haniewicz, R. D. Ferdman, P. C. Freire, D. J. Champion, K. A. Bunting, D. R. Lorimer, and M. A. McLaughlin, Mon. Not. R. Astron. Soc. **500**, 4620 (2020).

[80] Y. Sofue, M. Honma, and T. Omodaka, Publ. Astron. Soc. Jpn. **61**, 227 (2009), Complete data tables available online.

[81] J. I. Read, J. Phys. G **41**, 063101 (2014).

[82] R. N. Manchester, G. B. Hobbs, A. Teoh, and M. Hobbs, Astron. J. **129**, 1993 (2005).

[83] N. W. Evans, C. A. J. O'Hare, and C. McCabe, Phys. Rev. D **99**, 023012 (2019).

[84] P. J. McMillan, Mon. Not. R. Astron. Soc. **465**, 76 (2017).

[85] R. Abuter *et al.* (The GRAVITY Collaboration), Astron. Astrophys. **625**, L10 (2019).

[86] S. D. Bates, M. Bailes, N. D. R. Bhat, M. Burgay, S. Burke-Spolaor, N. D'Amico, A. Jameson, S. Johnston, M. J. Keith, M. Kramer *et al.*, Mon. Not. R. Astron. Soc. **416**, 2455 (2011).

[87] K. Kuijken and G. Gilmore, Mon. Not. R. Astron. Soc. **239**, 605 (1989).

[88] C. F. McKee, A. Parravano, and D. J. Hollenbach, Astrophys. J. Lett. **814**, 13 (2015).

[89] M. R. Buckley and A. H. G. Peter, Phys. Rep. **761**, 1 (2018).

[90] R. J. Jennings, D. L. Kaplan, S. Chatterjee, J. M. Cordes, and A. T. Deller, Astrophys. J. **864**, 26 (2018).

[91] C. M. F. Mingarelli, L. Anderson, M. Bedell, and D. N. Spergel, arXiv:1812.06262.

[92] https://github.com/R3zaEbadi/MW-Accelerometry.

[93] M. Pitkin, J. Open Source Softw. **3**, 538 (2018).

[94] D. Foreman-Mackey, J. Open Source Softw. **1**, 24 (2016).

[95] S. Chakrabarti, P. Chang, M. T. Lam, S. J. Vigeland, and A. C. Quillen, Astrophys. J. Lett. **907**, L26 (2021).

[96] S. A. Klioner *et al.* (Gaia Collaboration), arXiv:2012.02036.

[97] J. Bovy, arXiv:2012.02169.